A non-destructive method to calibrate the torsional spring constant of atomic force microscope cantilevers in viscous environments

Clodomiro Cafolla, Amir F. Payam, and Kislon Voïtchovsky

Citation: Journal of Applied Physics **124**, 154502 (2018); doi: 10.1063/1.5046648
View online: https://doi.org/10.1063/1.5046648
View Table of Contents: http://aip.scitation.org/toc/jap/124/15
Published by the American Institute of Physics

A non-destructive method to calibrate the torsional spring constant of atomic force microscope cantilevers in viscous environments

Clodomiro Cafolla,[1,a)] Amir F. Payam,[2,a)] and Kislon Voïtchovsky[1,b)]
[1]*Physics Department, Durham University, Durham DH1 3LE, United Kingdom*
[2]*Faculty of Engineering, University of Bristol, Bristol BS8 1TH, United Kingdom*

(Received 29 June 2018; accepted 21 September 2018; published online 17 October 2018)

Calibration of the torsional spring constant of atomic force microscopy cantilevers is fundamental to a range of applications, from nanoscale friction and lubrication measurements to the characterization of micro-electromechanical systems and the response of biomolecules to external stimuli. Existing calibration methods are either time consuming and destructive (*ex situ* static approaches), or rely on models using the frequency and quality factor (Q-factor) of the cantilever torsional resonance as input parameters (*in situ* dynamical approaches). While *in situ* approaches are usually preferred for their easy implementation and preservation of the cantilever, their dependence on the torsional resonance Q-factor renders calibration in highly viscous environments challenging. This is problematic, for example, in many nanoscale tribological applications. Here, we propose a calibration method that does not depend on the cantilever torsional Q-factor and show how the cantilever deflection can be converted into a lateral force. The method is tested with six cantilevers of different shapes and material composition and in six fluid media. The derived spring constants are compared with predictions from existing methods, demonstrating a higher precision, in particular, for highly viscous liquids.
https://doi.org/10.1063/1.5046648

INTRODUCTION

Atomic force microscopy (AFM) is a widely used tool for surface characterization, allowing both imaging at nanometer scales and measuring forces in the nano- to piconewton range.[1–3] While the most common AFM operation relies on measuring the flexural bending of a rectangular cantilever[4,5] that quantifies forces normal to a sample, torsional measurements are becoming increasingly popular for their ability to extract in-plane forces such as the frictional force with nanoscale lateral precision.[6–8] In torsional measurement, the sample is moved laterally with respect to the main axis of the cantilever, making the cantilever twist as the AFM tip rubs against the sample's surface. The shear force between the tip and the sample can be accurately determined from the twisting angle of the cantilever, provided that the torsional spring constant and the inverse optical lever sensitivity (InvOLS) of the system are known. The InvOLS is a constant depending on the geometry of the system and allows conversion of the raw photodiode measurement, taken in volts, into nanometer of lateral torsion at the tip.

While the flexural calibration of the cantilever is relatively straightforward (see, e.g., comprehensive reviews[9,10]), the torsional calibration is usually more complex and often cannot be achieved *in situ*, or without specialist, homebuilt equipment.[11–13] Methods for the calibration of torsional forces can be broadly classified into three main categories:[14] (i) theoretical,[15–17] (ii) static,[12,18–31] and (iii) dynamic.[14,32,33] Theoretical methods typically calculate the spring constant analytically from parameters characterizing the cantilever's geometry and its mechanical properties.[15–17] Such methods are particularly sensitive to errors originating from manufacturing variations in the cantilevers' dimensions and material properties. Static methods, in contrast, offer a direct measure of the lateral spring constant. They rely on a well-defined lateral force or displacement being applied to the AFM tip which generates torsional bending, thereby allowing the calculation of the torsional spring constant.[12,18–20] While static methods do not require many assumptions about the cantilever's geometry or material properties, they often require extra equipment and hard mechanical contact with a sample surface, leading to tip damage. These techniques are considered *ex situ* and hence more time consuming. Finally, dynamic calibration methods usually rely on the torsional resonance frequency of the cantilever to find its spring constant.[11,32,33]

Arguably, the best known torsional dynamic calibration methods are the so-called Cleveland method[32] and Sader method.[32–34] The Cleveland method measures the torsional frequency changes of the cantilever induced by the on-axis loading of added masses in order to deduce its torsional spring constant. In contrast, the Sader method determines the cantilever's torsional spring constant from its interaction with the surrounding medium, as quantified by the cantilever hydrodynamic function. The Sader method is particularly straightforward because it only requires the frequency and associated quality factor (Q-factor) of the cantilever torsional resonance as input parameters. As a result, the Sader method

[a)]C. Cafolla and A. F. Payam contributed equally to this work.
[b)]Author to whom correspondence should be addressed: kislon.voitchovsky@durham.ac.uk

has become one of the most popular approaches in the scientific community to calibrate microcantilevers. While highly successful in most common conditions, the dependence of the Sader method on the cantilever's hydrodynamic function can become problematic in viscous environments. Practically, this difficulty comes from the need to know the Q-factor of the cantilever, a quantity difficult to measure accurately in highly viscous liquids where the resonance can significantly broaden in the frequency domain. Additionally, the method assumes a Q-factor significantly larger than unity. This assumption, although commonly verified in air, tends to fail in liquids, especially for those with high viscosity.[33] As a result, the calculated torsional spring constant can vary significantly when derived in different viscous media, despite being an intrinsic property of the cantilever.[33] An alternative method that does not rely on the Q-factor is therefore highly desirable.

Here, we propose an alternative torsional calibration method that requires knowledge of four easily accessible parameters: the fundamental torsional resonance frequencies of a cantilever in air and in the medium of interest, and the cantilever width and length. Significantly, the method is independent of the cantilever Q-factor, non-destructive, and can be carried out on commercial AFMs without any further modifications. Since in most cases, the spring constant is only useful if the InvOLS is known, we adapt an existing InvOLS calibration methodology described elsewhere (Ref. 33) to also derive the system's InvOLS. The InvOLS calculation is based on the same four aforementioned parameters, on the Q-factor, and on the power spectrum density of the cantilever torsional motion at DC (P_{DC}), obtained from the cantilever's thermal torsional vibration spectrum. This allows for a more accurate value of the InvOLS because the quantity now depends on the inverse of the square root of the Q-factor, as opposed to the inverse of the Q-factor with the Sader formula. To validate our approach, we compare results derived with our method and the Sader method using different cantilevers in several media.

EXPERIMENTAL

The experimental section first derives expressions for the cantilever's torsional spring constant and InvOLS based on suitable observables. Secondly, all the details about the materials and methods of the experimental measurements are presented.

Theory

Let us consider a cantilever of length L, width b, and thickness h. Assuming that L is much greater than b and h, the torsional spring torque at the cantilever end is given by[32]

$$k_\phi = \frac{1}{3\pi^2}\rho_c h b^3 L \omega_{t,a}^2, \tag{1}$$

where ρ_c is the cantilever density and $\omega_{t,a}$ is the torsional resonance frequency of the cantilever in air. While it is possible to directly use Eq. (1) to calculate the torsional spring constant of the cantilever, there are in practice several important limitations. First, Eq. (1) requires knowledge of the cantilever thickness, a parameter that often carries a large variability with respect to the nominal value (see Fig. S1 in the supplementary material for a representative example). Second, this equation relies on the assumption of the cantilever's density being homogeneous. This is not always valid, with local inhomogeneities potentially affecting both the geometry and the density of the cantilever. We hence use the areal mass density in order to derive an effective cantilever density.

We assume, then, that the cantilever dynamics in a dense fluid can be described by a simplified hydrodynamic function of torsional motion $\Gamma_{tors}(\omega)$ characterized by two real (a_1, a_2) and one imaginary (b_1) regression coefficients as[35,36]

$$\Gamma_{tors}(\omega) \sim \left(a_1 + \frac{a_2}{\sqrt{Re}}\right) + j\left(\frac{b_1}{\sqrt{Re}}\right), \tag{2}$$

where a_1, a_2, and b_1 are the regression coefficients of the hydrodynamic function for the torsional motion of a rectangular cantilever in fluid environments. The values of a_1, a_2, and b_1 are 0.0634, 0.388, and 0.4, respectively.[35,36] Here, the fluid parameters are encapsulated by the Reynolds number, $Re = \rho_l \omega b^2/4\eta$, where ρ_l and η are the fluid density and viscosity, respectively. Using Eq. (2), we can relate the torsional resonance frequency of the cantilever in air, $\omega_{t,an}$, with that in liquid, $\omega_{t,fn}$, for any given vibration eigenmode, n:[32,37]

$$\omega_{t,fn}^2\left[\frac{3\pi a_1 \rho_f b}{2\rho_c h} + 1\right] + \omega_{t,fn}^{\frac{3}{2}}\left[\frac{6\pi a_2 \sqrt{\eta}\sqrt{\rho_f}}{2\rho_c h}\right] = \omega_{t,an}^2. \tag{3}$$

Using Eq. (3), the areal mass density of the cantilever, $\rho_c h$, can be calculated as follows:

$$\widehat{\rho_c h} = \frac{3\omega_{t,f1}^2 \pi a_1 \rho_f b + 6\pi a_2 \sqrt{\omega_{t,f1}^3 \rho_f \eta}}{2(\omega_{t,a1}^2 - \omega_{t,f1}^2)}. \tag{4}$$

Equation (4) can be used along with Eq. (1) to acquire the torsional torque constant (in Newton per radian) of the cantilever:

$$k_\phi = \frac{3\omega_{t,f1}^2 \pi a_1 \rho_f b^4 + 6\pi a_2 b^3 \sqrt{\omega_{t,f1}^3 \rho_f \eta}}{6\pi^2(\omega_{t,a1}^2 - \omega_{t,f1}^2)} L\omega_{t,a1}^2, \tag{5}$$

which requires the beam width and length and the torsional resonance frequencies in air and liquid as input parameters, alongside the density and viscosity of the fluid. The torsional spring constant (in N/m) of the cantilever can then be obtained from the torsional torque constant using the following equation:[33]

$$k_t = \frac{k_\phi L}{(L - \Delta L)h_t^2}, \tag{6}$$

where ΔL is the distance between the position of the tip and the end of cantilever and h_t is the tip height.

The spring constant can be used alongside the torsional InvOLS, γ, as formulated in Ref. 33, so as to multiply the cantilever deflection in volts and obtain the lateral force:

$$\gamma = h\sqrt{\frac{2k_B T}{\pi k_\phi f_o P_{DC} Q}}, \tag{7}$$

where k_B is Boltzmann's constant, T is the temperature, and

P_{DC} is the power spectrum density of the cantilever torsional motion at DC, measured on the cantilever's thermal torsional vibration spectrum.

Materials and methods

The frequency response of six commercially available cantilevers was investigated, each in six different media. The cantilevers were OMCL-RC800PSA (4 different cantilevers on the same chip, Olympus, Tokyo, Japan), AD-2.8AS (Adama Innovations LTD, Dublin, Ireland), and HQ-NSC18/HARD AL-BS (Windsor Scientific, Slough, UK). For clarity, the nominal geometrical and physical characteristics of the different cantilevers (hereafter referred to as C1–C6) are summarized in Table I.

Figure 1(a) highlights the different geometrical characteristics of the cantilevers used: C1-4 have a rectangular shape; C5 and C6 are a combination of a rectangle at the chip end and a triangle at the tip end.

As measurement media, we used air, ultrapure water, isopropanol, methanol, dimethyl sulfoxide (DMSO), hexadecane, and squalane. The ultrapure water (AnalaR Normapur) was purchased from VWR International Ltd (Lutterworth, UK). All other chemicals were purchased from Sigma-Aldrich (Dorset, UK) with a purity >99% and used without any further purification. The tabulated density and viscosity values of each fluid at the experimental temperature are shown in Table II.

The measurements were conducted on commercial Cypher ES AFM (Asylum Research, Santa Barbara, CA) equipped with a temperature-controlled sample stage. For each medium and for each cantilever, thermal spectra were recorded at 25 °C. To minimize any errors associated with changes in the laser alignment in different fluids, all the media were explored in the same session for each cantilever. When exchanging fluids within a given series, the tip was thoroughly washed with isopropanol (20 times with 100 μl) and then with the new solution of interest (40 times with 100 μl).

The frequency response of the cantilevers in the different media was investigated by recording the thermal spectrum of each cantilever in each medium. The Brownian motion of the fluid surrounding the cantilever results in naturally exciting the cantilever itself and determining a flexural and a torsional motion. The two different types of motion can be selectively detected using the AFM laser. Figure 1(b) schematically shows the different dynamics between flexural and torsional motion of the cantilever. The two motions result in different thermal spectra, as shown in Fig. 1(c). Tables S1–S6 in the

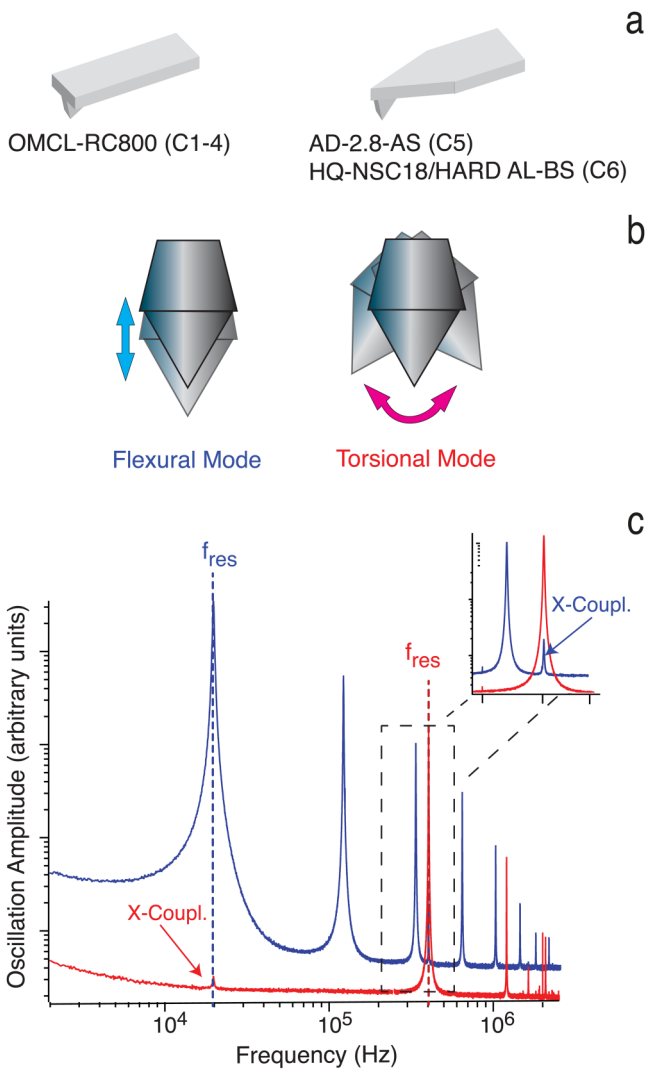

FIG 1. Cantilever types and calibration details for flexural vs torsional modes. (a) Geometry of the cantilevers used in the study. (b) Pictorial representation of the different motion of the cantilever in flexural and torsional modes. (c) Representative example of flexural (blue) and torsional (red) thermal spectra for a given cantilever. In each case, the resonance frequency, f_{res}, of the first eigenmode is shown. Cross coupling between the two modes is negligible for our purposes.

TABLE I. Summary of the characteristics of the cantilevers (C1–C6) used for this study.

Cantilever	Commercial name	Length (μm)	Width (μm)	Tip height (μm)	Material
C1	OMCL-RC800PSA	100.0	20.0	2.9	Silicon nitride
C2	OMCL-RC800PSA	100.0	40.0	2.9	Silicon nitride
C3	OMCL-RC800PSA	200.0	20.0	2.9	Silicon nitride
C4	OMCL-RC800PSA	200.0	40.0	2.9	Silicon nitride
C5	AD-2.8-AS	225.0	35.0	12.5	Diamond
C6	HQ-NSC18/HARD AL-BS	225.0	27.5	15.0	Diamond-like carbon

TABLE II. Density and viscosity values for all the media[38–40] at 25 °C.

Medium	Density (kg/m^3)	Viscosity (Pa s)
Air	1.18	1.83×10^{-5}
Methanol	787.00	5.43×10^{-4}
Water	998.00	8.90×10^{-4}
DMSO	1095.00	1.99×10^{-3}
Isopropanol	785.00	2.10×10^{-3}
Hexadecane	769.00	3.08×10^{-3}
Squalane	805.00	2.80×10^{-2}

supplementary material provide a detailed summary of the frequency responses of the cantilevers in the different media.

RESULTS AND DISCUSSION

Figure 2 compares the new method proposed here with the Sader method. Representative results are given for the spring constant of cantilever C3 in all the six fluids.

For all the cantilevers studied, we found our method to be significantly less sensitive to viscosity in determining the spring constant. The robustness of our approach is particularly obvious in highly viscous media [Fig. 2(a)] where the dependence of the Sader method on the cantilever Q-factor hinders predictions. Accurate determination of the Q-factor is strongly dependent on the fitting interval selected in the thermal spectrum, especially since Q may be close to unity[33] [Fig. 2(b)]. In the case of C2 and C6 (see supplementary material, Figs. S2 and S5), our method appears more robust than the Sader method also in low viscous media. This is not surprising since the Sader method relies on the assumption of a Q-factor much greater than unity, a condition which is typically met for stiff cantilevers in air.[32,33,44] However, applying the method can be challenging even in media with viscosity as low as water.[33]

As illustrated in Fig. 2(a) and Figs. S2–S6 and Tables S1–S6 (supplementary material), the proposed approach shows also greater precision in comparison with the Sader method: for highly viscous media, the error is significantly smaller and, in some cases, reduced up to four times. For cantilevers C5-6 (Figs. S5 and S6 and Tables S5 and S6 in the supplementary material), the uncertainty is smaller in all the media considered.

In order to quantitatively assess the robustness of our method, we calculated the relative variability of predictions for each cantilever across the different media (Fig. 3). Here, the relative variability is defined as the difference between the maximum and the minimum spring constant normalized by the average value. The results clearly confirm the robustness of our method against the impact of the surrounding fluid's viscosity with the normalized variability range being, in some cases, even more than 4 times smaller with the proposed method. In Fig. 3(b), we consider a reduced set excluding the highest viscosity data point (squalane) given its possible biasing of the results. Again, our method remains significantly less sensitive to viscosity changes in comparison with the Sader method. Further statistical data analysis on the spring constant variability is available in the supplementary material (Fig. S7).

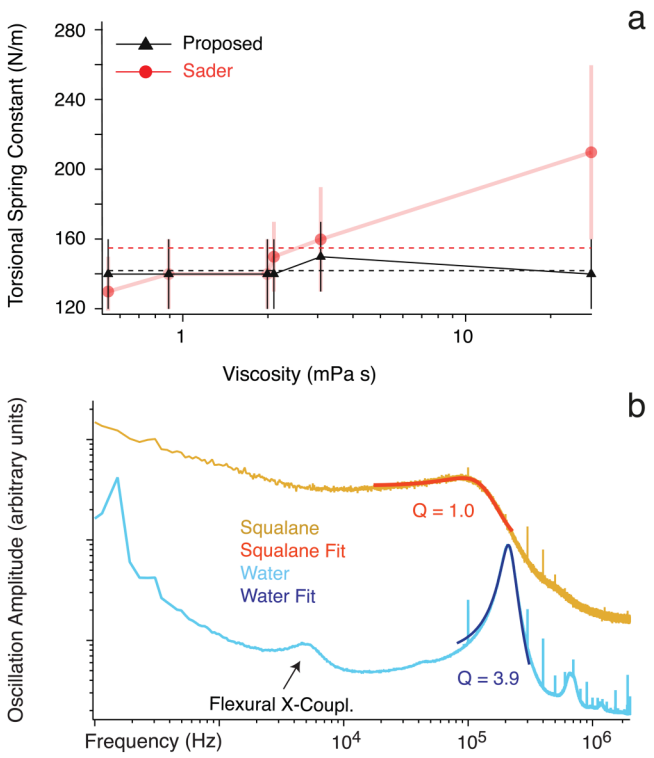

FIG 2. (a) Comparison of predictions derived with the proposed method and the Sader method in fluids of varying viscosity for cantilever C3 used as an example. The dashed lines represent the average spring constant for each method. The proposed method appears more precise considering its smaller deviation from the mean value. Predictions from the Sader method are significantly more dependent on viscosity variations between media. See Figs. S2–S6 in the supplementary material for the results obtained with the other cantilevers. (b) Representative thermal spectra in low and high viscosity media (water and squalane, respectively). In both cases, the first eigenmode is fitted with the thermal noise method.[4,5,33,41–44] In high viscosity media, the Q-factor significantly decreases and approaches unity, rendering the fitting procedure prone to large variations in the derived Q value depending on the fitting interval. Error bars in (a) are calculated using standard formulae for error propagation (see supplementary material, Sec. 3). The data points and error bars relative to the Sader method have been shadowed and enlarged so as to enhance graph readability. The thermal spectrum of squalane in (b) has been offset vertically for clarity.

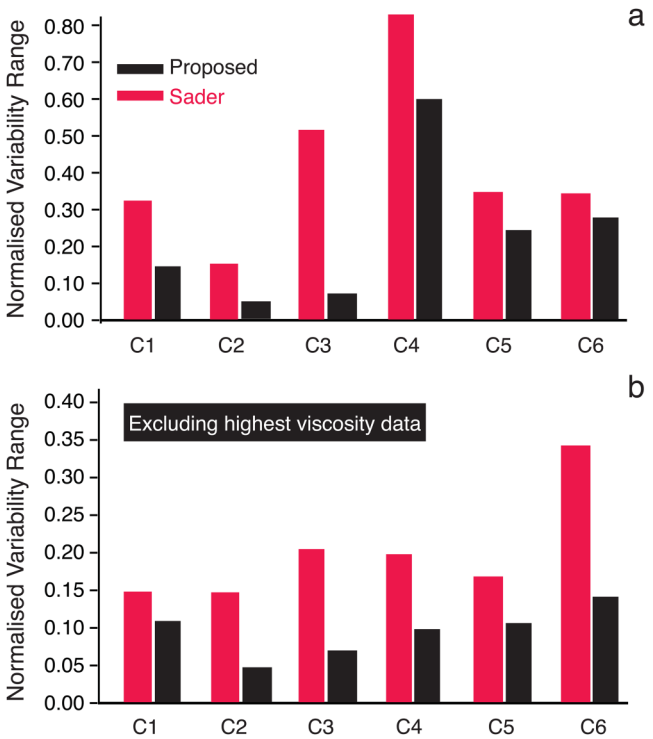

FIG 3. Quantification of the variability across media for each cantilever's torsional spring constant for the proposed and the Sader methods. In (a), the variability is calculated using the data in all the media, whereas in (b) we have excluded the data relative to the highest viscosity medium (squalane). For each cantilever, the variability of the spring constant across media is calculated as the difference between the maximum and the minimum spring constant normalized by the average value.

Our method could, in principle, be extended to the calibration of arbitrarily shaped cantilevers, but this would require a prior determination of an effective cantilever width from a torsional perspective. This task is non-trivial with, to the best of our knowledge, no simple existing approach for calculating the effective width. Attempts to calibrate the torsional spring constant of a triangular cantilever confirmed that our method tends to be more robust against the influence of viscosity variability, but the values derived are partly speculative for the lack of a reliable input (effective width) and the absence of independent comparative measurements (see Sec. 5 of the supplementary material).

Combining Eqs. (5) and (7), it is possible to calculate easily the torsional InvOLS of the cantilevers, thereby allowing a straightforward derivation of the lateral shear force experienced by the AFM tip. Our method would hence also potentially increase the accuracy of the torsional InvOLS calculation. This is because in our method the torsional InvOLS depends on the inverse of the square root of the Q-factor, whereas in currently used models there is a linear dependence of the InvOLS on the inverse of the Q-factor.[33] We note that our method relies on knowledge of P_{DC} from the thermal spectrum of the cantilever. While the value of P_{DC} can be readily obtained in most commercial AFMs, it is worth mentioning that additional gains and filters are often applied to the lateral deflection signal by commercial software in default settings. This may lead to an unexpectedly high or low InvOLS due to the P_{DC} value being incorrect.

CONCLUSIONS

In this paper, we present a non-destructive and non-invasive method to determine the torsional spring constant of a cantilever and to calculate the lateral shear force experienced by the AFM tip from the raw deflection as obtained from the photodetector. The method requires the following input parameters: the fundamental torsional resonance frequencies of the cantilever in air and in the medium of interest, and the cantilever width and length. Significantly, the method is independent of the cantilever Q-factor which renders our method particularly effective in high viscosity media. We validate our approach with cantilevers exhibiting different geometries and in six different media. Our method can be carried out on commercial AFMs without the need for any extra equipment. We believe that the proposed method could be particularly useful for quantitative high-resolution torsional imaging in solution[45] and in the field of nanoscale friction and tribology, for example, when investigating ionic liquids,[46] organic lubricants,[6] surfactants layers,[47] and functional nano-interfaces.[48] In order to facilitate the use of our method, the script of a Python code capable of calculating the torsional spring constant, its uncertainty, and the torsional InvOLS using the proposed method is given in the last section of the supplementary material.

SUPPLEMENTARY MATERIAL

See supplementary material for the EM analysis of the tips, the frequency response of each cantilever in the different media including a fully triangular cantilever, and detailed error calculations and statistical analysis of the results. The Python code used to calculate the torsional spring constants is also presented in full.

ACKNOWLEDGMENTS

The authors acknowledge funding from the Engineering and Physical Sciences Council (ICASE studentship, Grant No. EP/P510476/1), the Biotechnology and Biological Science Research Council (Grant No. BB/M024830/1), and the European Council (FP7 CIG 631186). Insightful discussions with Mr. William J. Trewby are gratefully acknowledged. The authors acknowledge Dr. Budhika Mendis and Mr. Leon Bowen for their invaluable suggestions on scanning electron microscopy.

[1]J. M. Fernandez and H. Li, Science **303**, 1674 (2004).
[2]M. Grandbois, M. Beyer, M. Rief, H. Clausen-Schaumann, and H. E. Gaub, Science **283**, 1727 (1999).
[3]R. García, R. Magerle, and R. Perez, Nat. Mater. **6**, 405 (2007).
[4]M. J. Higgins, R. Proksch, J. E. Sader, M. Polcik, S. Mc Endoo, J. P. Cleveland, and S. P. Jarvis, Rev. Sci. Instrum. **77**, 013701 (2006).
[5]J. E. Sader, J. W. M. Chon, and P. Mulvaney, Rev. Sci. Instrum. **70**, 3967 (1999).
[6]K. Voïtchovsky, Nanoscale **8**, 17472 (2016).
[7]T. D. Li and E. Riedo, Phys. Rev. Lett. **100**, 106102 (2008).
[8]C. Cafolla and K. Voïtchovsky, Nanoscale **10**, 11831 (2018).
[9]C. T. Gibson, A. Smith, and C. J. Roberts, Nanotechnology **16**, 234 (2005).
[10]M. L. B. Palacio and B. Bhushan, Crit. Rev. Solid State Mater. Sci. **35**, 73 (2010).
[11]M. Munz, J. Phys. D **43**, 063001 (2010).
[12]R. J. Cannara, M. Eglin, and R. W. Carpick, Rev. Sci. Instrum. **77**, 053701 (2006).
[13]K.-H. Chung, J. R. Pratt, and M. G. Reitsma, Langmuir **26**, 1386 (2010).
[14]J. D. Parkin and G. Hähner, Nanotechnology **25**, 225701 (2014).
[15]R. Álvarez-Asencio, E. Thormann, and M. W. Rutland, Rev. Sci. Instrum. **84**, 096102 (2013).
[16]J. M. Neumeister and W. A. Ducker, Rev. Sci. Instrum. **65**, 2527 (1994).
[17]J. L. Hazel and V. V. Tsukruk, J. Tribol. **120**, 814 (1998).
[18]M. G. Reitsma, R. S. Gates, L. H. Friedman, and R. F. Cook, Rev. Sci. Instrum. **82**, 093706 (2011).
[19]E. Liu, B. Blanpain, and J. P. Celis, Wear **192**, 141 (1996).
[20]E. Tocha, J. Song, H. Schönherr, and G. J. Vancso, Langmuir **23**, 7078 (2007).
[21]A. Feiler, P. Attard, and I. Larson, Rev. Sci. Instrum. **71**, 2746 (2000).
[22]G. Bogdanovic, A. Meurk, and M. W. Rutland, Colloids Surf. B **19**, 397 (2000).
[23]H. Xie, J. Vitard, S. Haliyo, and S. Régnier, Rev. Sci. Instrum. **79**, 096101 (2008).
[24]M. G. Reitsma, Rev. Sci. Instrum. **78**, 106102 (2007).
[25]D. F. Ogletree, R. W. Carpick, and M. Salmeron, Rev. Sci. Instrum. **67**, 3298 (1996).
[26]D. Choi, W. Hwang, and E. Yoon, J. Microsc. **228**, 190 (2007).
[27]M. Varenberg, I. Etsion, and G. Halperin, Rev. Sci. Instrum. **74**, 3362 (2003).
[28]X. Ling, H. J. Butt, and M. Kappl, Langmuir **23**, 8392 (2007).
[29]D. B. Asay and S. H. Kim, Rev. Sci. Instrum. **77**, 043903 (2006).
[30]S. Ecke, R. Raiteri, E. Bonaccurso, C. Reiner, H. J. Deiseroth, and H. J. Butt, Rev. Sci. Instrum. **72**, 4164 (2001).
[31]R. G. Cain, M. G. Reitsma, S. Biggs, and N. W. Page, Rev. Sci. Instrum. **72**, 3304 (2001).
[32]C. P. Green, H. Lioe, J. P. Cleveland, R. Proksch, P. Mulvaney, and J. E. Sader, Rev. Sci. Instrum. **75**, 1988 (2004).
[33]N. Mullin and J. K. Hobbs, Rev. Sci. Instrum. **85**, 113703 (2014).
[34]C. P. Green and J. E. Sader, J. Appl. Phys. **92**, 6262 (2002).
[35]T. Cai, ProQuest Dissertations Publishing 3601316, 1 (2013).

[36]T. Cai, F. Josse, S. Heinrich, N. Nigro, I. Dufour, and O. Brand, *2012 IEEE International Frequency Control Symposium* (IEEE, 2012), p. 1.
[37]C. A. Van Eysden and J. E. Sader, J. Appl. Phys. **100**, 114916 (2006).
[38]J. Kestin, M. Sokolov, and W. A. Wakeham, J. Phys. Chem. Ref. Data **7**, 941 (1978).
[39]H. D. Young and R. A. Freedman, University Physics with Modern Physics (Pearson, 2012).
[40]See https://wiki.anton-paar.com/en/tables/ for Tables: Anton Paar Wiki; accessed 22 June 2018.
[41]J. L. Hutter and J. Bechhoefer, Rev. Sci. Instrum. **64**, 1868 (1993).
[42]H. J. Butt and M. Jaschke, Nanotechnology **6**, 1 (1995).
[43]S. M. Cook, T. E. Schäffer, K. M. Chynoweth, M. Wigton, R. W. Simmonds, and K. M. Lang, Nanotechnology **17**, 2135 (2006).
[44]T. Pirzer and T. Hugel, Rev. Sci. Instrum. **80**, 035110 (2009).
[45]N. Mullin and J. K. Hobbs, Phys. Rev. Lett. **107**, 197801 (2011).
[46]F. Endres, N. Borisenko, S. Z. El Abedin, R. Hayes, and R. Atkin, Faraday Discuss. **154**, 221 (2012).
[47]R. Atkin and G. G. Warr, JACS **127**, 11940 (2005).
[48]K. Voïtchovsky, D. Giofre, J. J. Segura, F. Stellacci, and M. Ceriotti, Nat Commun. **7**, 13064 (2016).